e-ISSN 1734-9168
http://www.isez.pan.krakow.pl/en/folia-biologica.html

Folia Biologica (Kraków), vol. 70 (2022), No 4
https://doi.org/10.3409/fb_70-4.20

In vitro Sodium Fluoride Treatment Significantly Affects Apoptosis and Proliferation in the Liver of Embryonic Chickens

Agnieszka K. GRZEGORZEWSKA, Dorota WOJTYSIAK, Klaudia JASZCZA, and Andrzej SECHMAN

Accepted October 18, 2022 *Published online November 16, 2022* *Issue online December 06, 2022*

Original article

GRZEGORZEWSKA A.K., WOJTYSIAK D., JASZCZA K., SECHMAN A. 2022. *In vitro* sodium fluoride treatment significantly affects apoptosis and proliferation in the liver of embryonic chickens. Folia Biologica (Kraków) **70**: 163-175.

Sodium fluoride (NaF), although helpful in preventing dental decay, may negatively affect the body. The aim of this study was to examine the effects of a 6-h *in vitro* treatment of livers isolated from 14-day-old chicken embryos with NaF at doses of 1.7 (D1), 3.5 (D2), 7.1 (D3) and 14.2 mM (D4), with regard to apoptosis, cell proliferation and tissue structure. The mRNA expression of the apoptosis regulators *CYCS*, *APAF1*, *BCL2*, *CASP3*, *CASP9* and *TMBIM1* was analysed by the qPCR method. Apoptotic cells were detected by a TUNEL assay. The tissue and DNA structure were also analysed by histological staining (H&E, Feulgen). The number of proliferating cells was determined and the apoptosis regulatory proteins were localised by the immunohistochemical staining of PCNA, CASP3 and APAF1. The results showed that the mRNA expression of *CYCS*, *BCL2*, *CASP3*, *CASP9* and *APAF1* increased significantly in the D1 group, as did that of *CASP9* in the D3 group and of *BCL2* and *APAF1* in the D4 group. The number of apoptotic cells increased significantly in the D4 group, where they increased from 18% to 49%. On the other hand, the number of proliferating cells decreased gradually, in a dose-dependent manner, from 84% in the control group to 5.5% in the D4 group. The expression of apoptosis-regulating factors also increased: in the D3 and D4 groups, the CASP3 immunopositive reaction was more intensive in single cells in the embryonic livers, whereas that of APAF1 increased in the hepatocytes as well as in the hepatic blood vessel walls. The mechanism of the effect of NaF on apoptosis in the embryonic liver is very complex. In the groups exposed to higher doses of NaF, apoptosis was significantly stimulated, while proliferation was inhibited and the tissue structure was damaged. The expression of apoptosis regulators at the mRNA and protein levels increased, but the mRNA expression did not depend on the NaF dose. These results reveal that NaF, by changing the balance between apoptosis and the proliferation of hepatocytes, may disturb the development and function of the liver in embryonic chickens. Therefore, the risk of exposure to NaF should be considered when determining the standards for human and animal exposure to this compound.

Key words: NaF, bird, liver, toxicity, cell death.

Agnieszka K. GRZEGORZEWSKA✉, Klaudia JASZCZA, Andrzej SECHMAN, Department of Animal Physiology and Endocrinology, University of Agriculture in Krakow, Al. Mickiewicza 24/28, 30-059 Kraków, Poland.
E-mail: a.grzegorzewska@ur.krakow.pl
Dorota WOJTYSIAK, Department of Animal Genetics, Breeding and Ethology, University of Agriculture in Krakow, Al. Mickiewicza 24/28, 30-059 Kraków, Poland.

Fluorine commonly occurs in the environment. Natural sources such as rock erosion, local industries (chemical, glass and enamel industries), as well as farms where phosphorus fertilisers are widely used, affect the level of fluorine in the ground and water. In addition, fluorides comprised of inorganic and organic fluorine compounds are contained in dental products for the prevention and remineralisation of dental caries (GRIFFIN *et al.* 2007). Low-dose fluorides are beneficial to the bone condition and have been used in the case of advanced osteoporosis. However, excessive systemic exposure to fluorides can lead to skeletal or dental fluorosis (FORDYCE 2011). The toxic dose of fluoride is 5 mg/kg b.w.

(EKSTRAND *et al.* 1981). Acute and high-dose exposure to fluorides can also induce oxidative stress (CAO *et al.* 2015) and can cause renal disfunction (LANTZ *et al.* 1987), reproductive toxicity (GUPTA *et al.* 2007) and infertility (FRENI 1994). Moreover, a high dose of fluoride, due to its ability to cross the placental barrier, may directly damage a developing mammalian foetus (GUNA SHERLIN & VERMA 2001). The kidney eliminates 50-80% of the absorbed fluoride (GUAN *et al.* 2000), but the liver, as a site of very active metabolism, is especially susceptible to fluoride toxicity (XIONG *et al.* 2007). Exposure to excessive fluoride induces damage in the liver and kidneys (SHIVASHANKARA *et al.* 2000). It is believed that waterborne fluoride may affect the liver and kidney functions in animals and humans in a dose-dependent manner (GUAN *et al.* 2000).

Apoptosis, or programmed cell death, is a key process in regulating the maturation, remodelling, growth and development of a living organism. It has been detected in chickens as early as 3 h after the onset of incubation (HIRATA & HALL 2000). Apoptosis can be triggered through different intracellular signalling pathways. To maintain tissue homeostasis, many regulatory and inhibitory mechanisms must play a role in controlling apoptosis. Caspases (CASP) are a family of intracellular cysteine proteases that are linked to both the initial and final stages of apoptosis. In birds, as in other animals, the orthologous caspase mRNAs have been characterised (chicken CASP1, CASP2, CASP3, CASP6, CASP7, CASP8, CASP9, CASP10, CASP14 and CASP18) and two general pathways involving initiator caspases have been identified. One upstream pathway, which is promoted by the activation of death receptors, results in the processing of the initiator CASP8 and/or CASP10 (STRASSER & NEWTON 1999). The alternative pathway involving an initiator caspase occurs after the release of mitochondrial cytochrome C (EKERT *et al.* 2001). Cytosolic cytochrome C mediates the formation of the apoptosome complex, which is a high-molecular-weight complex consisting of APAF1 and CASP9. The autoactivation of either caspase-8 or caspase-9 eventually initiates the processing of an effector caspase (CASP3, CASP6 or CASP7) and the full potentiation of the caspase cascade. Caspase activation is regulated by the cellular pro- and anti-apoptotic BCL2 family of proteins. In particular, anti-apoptotic members of the BCL2 family, such as BCL2, form ion channels within the mitochondrial membrane and help to maintain mitochondrial integrity. In the past few years, a novel group of cell death regulators have emerged, known as the Transmembrane BAX Inhibitor-1 Motif-containing (TMBIM) protein family. This group of proteins is composed of at least six highly-conserved members that are expressed in mammals, with homologues in insects, fish, plants, viruses and yeast. Different studies indicate that all TMBIM family members exert inhibitory activities in different settings of apoptosis. TMBIM1 affects the apoptosis signalling induced by FasL (ROJAS-RIVERA & HETZ 2015).

In our previous study, we found that an *in vitro* sodium fluoride (NaF) treatment significantly affected the mRNA expression and immunoexpression of oxidative stress regulatory enzymes in the embryonic gonads of chickens (GRZEGORZEWSKA *et al.* 2020b). NaF may also affect the expression of steroid hormone receptors in an embryonic chicken's ovaries and testis (GRZEGORZEWSKA 2020). We also demonstrated that chicken embryos may be used as an animal model in studies concerning NaF embryotoxicity. There are many reports concerning the effects of environmental factors on apoptosis in an embryonic chicken's liver. They have revealed that electromagnetic fields (LAHIJANI *et al.* 2011), zinc oxide nanoparticles (HAO *et al.* 2017) or aflatoxin b1 (AFB1) (ELWAN *et al.* 2021) may all induce apoptosis in the livers of chicken embryos, but the effects of NaF on apoptosis and proliferation in the embryonic liver have not been fully elucidated. The aim of this study, therefore, was to analyse the effects of an *in vitro* treatment of embryonic chicken livers with increasing doses of NaF on the tissue structure, number of apoptotic cells, proliferation index and the immunolocalisation of APAF1 and CASP3, as well as on the mRNA expression of apoptosis regulatory proteins.

Research hypothesis: Exposure of embryonic livers from chickens to NaF will affect the tissue structure and the expression of apoptosis regulators.

Materials and Methods

Ethics approval

The chicken embryo and CAM model may be used as an alternative model and does not require the approval of a Local Ethics Committee (Directive 2010/63/EU of the European Parliament and of the Council of 22 September 2010 on the protection of animals used for scientific purposes).

Reagents

Chemicals used for the liver tissue *in vitro* treatment: Eagle's medium (Biomed, Lublin, Poland); Bovine serum albumin and Antibiotic-antimycotic solution (with 10,000 units of penicillin, 10 mg streptomycin and 25 µg amphotericin B per ml (Merck KGaA, Darmstadt, Germany); and NaF (Sigma, St. Louis, MO, USA).

The chemicals used in the tissue preparation and the Real-time PCR analysis were purchased from the following companies: StayRNA (A&A Biotechnology,

Gdynia, Poland); TRI-Reagent (MRC Inc., Cincinnati, OH, USA), High-Capacity cDNA Reverse Transcription Kit (ThermoFisher Scientific, Waltham, MA, USA); primers (IBB PAN, Warsaw, Poland); 5x HOT FIREPol EvaGreen qPCR Mix Plus (ROX) (Solis BioDyne, Tartu, Estonia).

The chemicals used for the immunohistochemistry were: ApopTag Plus Peroxidase *in situ* Apoptosis Detection Kit (Millipore, Temecula, MA,USA); Rabbit anti-Caspase 3 polyclonal antibody (PA5-23921; ThermoFisher Scientific, Waltham, MA, USA); APAF1 Recombinant Rabbit Monoclonal Antibody (SY22-02) (MA5-32082, Invitrogen, ThermoFisher Scientific, Waltham, MA, USA); PCNA Polyclonal Antibody (PA1-38424, ThermoFisher Scientific, Waltham, MA, USA); Metal Enhanced DAB Substrate Kit (ThermoFisher Scientific, Waltham, MA, USA); DyLight 594 Anti-Rabbit IgG (H+L), VECTASHIELD® Hardset™ Antifade Mounting Medium with DAPI; Normal goat serum and haematoxylin QS (Vector Laboratories, Burlingame, CA, USA).

All other reagents were obtained from Sigma (St. Louis, MO, USA) POCH (Gliwice, Poland) or Warchem (Marki, Poland).

Animals and the experimental procedure

The experiment was conducted on n=60 fertilised eggs of Hy Line chickens purchased from a local breeder (Tarnów, Poland).

The eggs were incubated in a Brinsea 190 Advance automatic incubator under standard conditions (temp. 37.5°C; humidity 55%). On the 8th day of incubation, the quality of the eggs was controlled during an observation (candling) by ovoscope, and the unfertilised eggs and dead embryos were eliminated. On the 14th day of embryogenesis, the embryos were sacrificed and the total livers were isolated.

In the case of chickens, the left lobe of the liver is divided into two parts (middle and lateral), while the gallbladder is located on the surface of the right lobe. Therefore, the livers were isolated very carefully, to avoid damaging the gallbladder. The livers were then dissected, immediately placed in ice-cold PBS, and rinsed twice with PBS containing an antibiotic-antimycotic solution. Each lobe of the liver was put into the well of 24-well plates containing 1 ml of Eagle's medium, supplemented with a 0.05% bovine serum albumin and 2 µl antibiotic antimycotic solution, and with NaF at concentrations of 1.7, 3.5, 7.1 or 14.2 mM, or a vehicle (Eagle's medium with a NaF solvent – H_2O). The liver lobes were incubated separately, with the left lobe used for further immunohistochemical analyses (n=6 in each group), and the right lobe used for the qPCR analyses (n=6 in each group). The livers were cultured for 6 h at 38°C in a humidified atmosphere of 95% air and 5% CO_2. The concentration of NaF in the medium was established by considering the research data (WEI *et al.* 2014; FU *et al.* 2016) and as tested by us previously in other experiments (GRZEGORZEWSKA 2020a; GRZEGORZEWSKA *et al.* 2020b).

Following incubation, the tissue samples were immediately placed in StayRNA and were stored at -20°C until total RNA isolation, or were fixed in a freshly prepared 10% (v:v) buffered formalin pH=6.9, then processed and embedded in paraffin wax for the subsequent histological analysis, DNA staining, localisation, counting of the apoptotic and proliferating cells, and the immunodetection of CASP3 and APAF1.

RNA extraction, reverse transcription and real-time PCR

The RNA isolation and reverse transcription were conducted as described previously (GRZEGORZEWSKA *et al.* 2020a), and the EvaGreen real-time PCR analyses were performed according to the manufacturer's instructions. Briefly, the total RNA (2 µg from each tissue extracted with TRI-reagent) was reverse-transcribed with a High-Capacity cDNA Reverse Transcription Kit including random primers. The samples were incubated in a thermocycler (Mastercycler Gradient; Eppendorf, Hamburg, Germany). in accordance with the following thermal profile: 25°C for 10 min, 37°C for 120 min and 85°C for 5 min. The obtained cDNA was used in a real-time qPCR for cytochrome C (*CYCS*), *APAF1*, Transmembrane BAX Inhibitor Motif Containing 1 (*TMBIM1*), *BCL2*, caspase-3 (*CASP3*), caspase-9 (*CASP9*), and for glyceraldeyde-3-phosphate dehydrogenase (*GAPDH*) as a housekeeping gene. The amplifications were performed in a 96-well thermocycler (StepOnePlus; Applied Biosystems, USA), according to the following recommended cycling programme: 15 min at 95°C, 40 cycles of 15 s at 95°C, 20 s at 62°C and 20 s at 72°C. The primers (Table 1) were synthesised according to previously used and tested sequences (YIN *et al.* 2016; KHILLARE *et al.* 2018). The singleplex real-time qPCRs for the examined genes were performed in a 10 µl volume containing: 2 µl 5x HOT FIREPol EvaGreen qPCR Mix Plus, 0.12 µl Primer Forward (10 pmol/µl), 0.12 µl Primer Reverse (10 pmol/µl), 1 µl cDNA (10x diluted sample after the RT template) and PCR grade H_2O up to 10 µl. Each sample was analysed in duplicate. A no-template control was included in each run. A relative quantification of the examined genes was calculated after a normalisation with the GAPDH transcript and by employing the expression in the liver tissue of the control chickens as the calibrator by using the $2^{-\Delta\Delta Ct}$ method (LIVAK & SCHMITTGEN 2001). A quantification was performed using StepOne integrated software.

Table 1

Positions of oligonucleotide primers in the mRNA sequence, GenBank Accession Numbers, sequences of amplified gene primers, annealing temperature of the PCR reaction and product size

Gene	Primer sequence (5'-3')	Position [bp]	GenBank Accession Number	Product size [bp]
APAF1	AAGGGCATAAGGAAGCAATCAA CAGCACAAGAAAGAACAGCACC	3269-3290 3402-3424	XM_416167.6	156
CYCS	TGTCCAGAAATGTTCCCAGTGC CCTTTGTTCTTATTGGCATCTGTG	33-54 147-170	NM_001079478	138
BCL2	GATGACCGAGTACCTGAACC CAGGAGAAATCGAACAAAGGC	679-698 772-792	NM_205339.2	114
CASP3	TGGCCCTCTTGAACTGAAAG TCCACTGTCTGCTTCAATACC	587-606 705-725	NM_204725.1	139
CASP9	CGAAGGAGCAAGCACGACAG CCGCAGCCCTCATCTAGCAT	99-118 209-228	AY057940	130
TMBIM1	TCCTCATCGCCATGCTCAT CCTTGGTCTGGAAGCAGAAGA	959-977 1007-1027	XM_4223067.4	69
GAPDH	GTGTGCCAACCCCCAATGTCTCT GCAGCAGCCTTCACTACCCTCT	752-774 827-848	NM_204305	97

CYCS – Cytochrome C, *APAF1* – Apoptotic protease activating factor 1, *BCL2* – B-cell lymphoma 2, *CASP3* – Caspase 3, *CASP9* – Caspase 9, *TMBIM1*– transmembrane BAX inhibitor motif containing 1, *GAPDH* – Glyceraldehyde 3-phosphate dehydrogenase (housekeeping gene).

Immunohistochemical and histological analyses

H&E staining

For the histological analysis, deparaffinised and rehydrated 6-µm-thick sections of the chicken livers were stained according to the standard haematoxylin and eosin method: staining with a Harris Haematoxylin solution for 20 minutes, differentiation in 70% ethanol containing 1% HCl, and staining with an Eosin 1% aqua solution with acetic acid (according to Harris' Hematoxylin protocol, National diagnostics).

Feulgen staining – DNA detection

For the DNA detection, deparaffinised and rehydrated 6-µm-thick sections of the chicken livers were stained according to the protocol for Feulgen staining. Acid hydrolysis was performed with a HCl solution. The next step was a treatment with Schiff's reagent and differentiation with sodium sulphite (MELLO & VIDAL 2017).

TUNEL assay

For the evaluation of apoptosis, the chicken livers were fixed in 4% formaldehyde in phosphate-buffered saline (pH 7.4) and were embedded in paraffin wax by a routine procedure. Deparaffinised and rehydrated 6-µm-thick sections of the liver tissues were incubated with proteinase K (20 µg ml^{-1}) in 10 mM Tris-HCl, pH 7.4 at 37°C for 20 min. Apoptotic cells were detected by TUNEL (GAVRIELI *et al.* 1992; GRZEGORZEWSKA *et al.* 2020a) using an *in situ* cell death detection kit, POD according to the manufacturer's instructions (Roche Diagnostics GmbH, Mannheim, Germany). Negative controls were prepared by incubation without terminal deoxynucleotidyl transferase. To visualise the immunoreaction products, sections were incubated with a DAB and H_2O_2 mixture for approximately 2 min. The slides were examined under an Axio Scope light microscope with an Axiocam 503 colour camera and ZEN 2.3 pro software (Carl Zeiss, Germany). The apoptotic cells (TUNEL-positive) were counted with a computerised image analysis system on 10-15 random areas of each liver tissue and were averaged for each embryo. The resulting value (the apoptotic index: AI) was shown as the number of TUNEL-positive cells per 100 cells counted. The mean value was calculated from a total of six embryos.

Immunohistochemical localisation of CASP3, APAF1 and PCNA

The liver tissue sections (6 µm thick) were deparaffinised in xylene and rehydrated by passing through an alcohol gradient, then rinsed in water and heated in a citrate buffer (pH 6.0, 75°C, 20 min), followed by incubation with 5% (v/v) normal goat serum in TBST at room temperature for 30 min. The sections were then incubated overnight (4°C) with specific antibodies: Rabbit anti-Caspase 3 polyclonal antibody, dilution 1:150 (PA5-23921; ThermoFisher Scientific, Waltham, MA, USA); APAF1 Recombinant Rabbit Monoclonal Antibody, dilution 1:150 (SY22-02) (MA5-32082, Invitrogen, ThermoFisher Scientific, Waltham, MA, USA); and PCNA Polyclonal Antibody, dilution 1:100 (PA1-38424, ThermoFisher Scientific, Waltham, MA, USA). They were then washed with

TBS, incubated with the fluorescent secondary antibody DyLight 594 Anti-Rabbit IgG (H+L) (2 h, darkness) and mounted with a VECTASHIELD® Hardset™ Antifade Mounting Medium with DAPI. Negative controls were prepared by a replacement of the primary antibody with TBST. The slides were examined under an Axio Scope light microscope with an Axiocam 503 colour camera and ZEN 2.3 pro software (Carl Zeiss, Germany). The immunopositive reaction for APAF1 and CASP3 proteins was not localised in the cell nuclei, and it was estimated only as being strong, moderate, weak or very weak. The number of PCNA-positive cells was presented as the immunoreactivity, which represents the number of immunopositive cells (red fluorescence) per 100 cells (blue fluorescence of DAPI) in the selected area. The proliferating cells (PCNA-positive) were counted in the same manner as the apoptotic cells. The resulting value (the proliferation index: PI) was shown as the number of PCNA-positive cells per 100 cells counted. The mean value was calculated from n=6 embryos in each experimental group.

Statistical analysis

The gene expression data represents the mean relative quantity (RQ) from n=6 samples in each group. The analysis of the mRNA expression was performed in duplicate and standardised to control the expression in the liver (RQ = 1) using the $2^{-\Delta\Delta Ct}$ method (LIVAK & SCHMITTGEN 2001). The data was statistically analysed by one-way ANOVA (effect of treatment) followed by Duncan's multiple range test. Log transformations were performed as needed, to maintain the homogeneity of variance and normality. The values were expressed as means ± SEM and were considered significantly different at $p<0.05$. The calculations were performed using SigmaPlot (Systat Software Inc., San Jose, CA, USA).

Data and model availability statement

No data was deposited in an official repository. The data is available from the authors upon request.

Results

mRNA expression of the apoptosis regulators *CYCS*, *APAF1*, *TMBIM1*, *BCL2*, *CASP3* and *CASP9*

The expression of mRNA encoding *CYCS* increased significantly in the group exposed to 1.7 mM of NaF (D1), but in the other experimental groups, the levels of *CYCS* were not significantly different from those in the control group (Fig. 1A). The mRNA expression of *APAF1* was significantly higher in the D1, D3 and D4 NaF-treated groups (Fig. 1B). The *TMBIM1* mRNA expression in the embryonic chicken livers was not affected by NaF (Fig. 1C), whereas the antiapoptotic *BCL2* protein mRNA in-

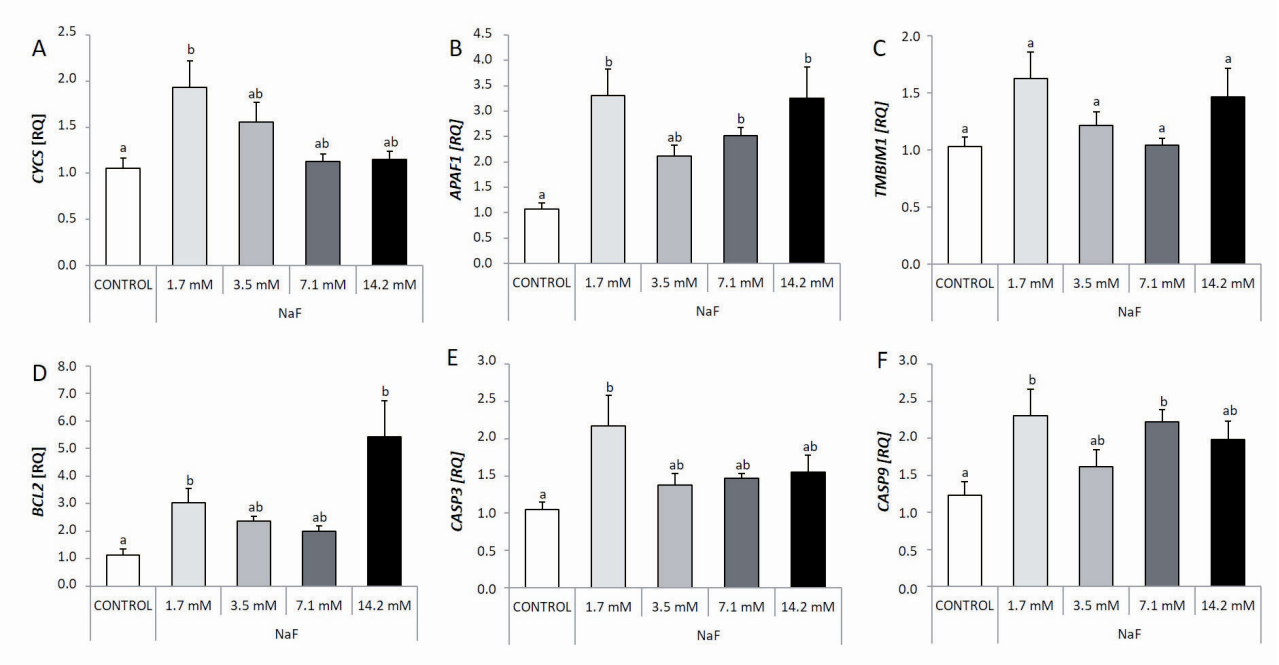

Fig. 1. mRNA expression of genes encoding the apoptosis regulators *CYCS*, *APAF1*, *BCL2*, *CASP3*, *CASP9 and TMBIM1*, with *GAPDH* as a reference gene, in the liver tissues of chicken embryos in the control group and following an *in vitro* treatment with 1.7 (D1), 3.5 (D2), 7.1 (D3) and 14.2 mM (D4) NaF. Each value represents the mean ± SEM from n = 6 (six embryonic livers). The gene expression data represents the mean relative quantity (RQ) standardised to control the expression in the liver (RQ = 1). Values marked with different letters differ significantly ($p<0.05$).

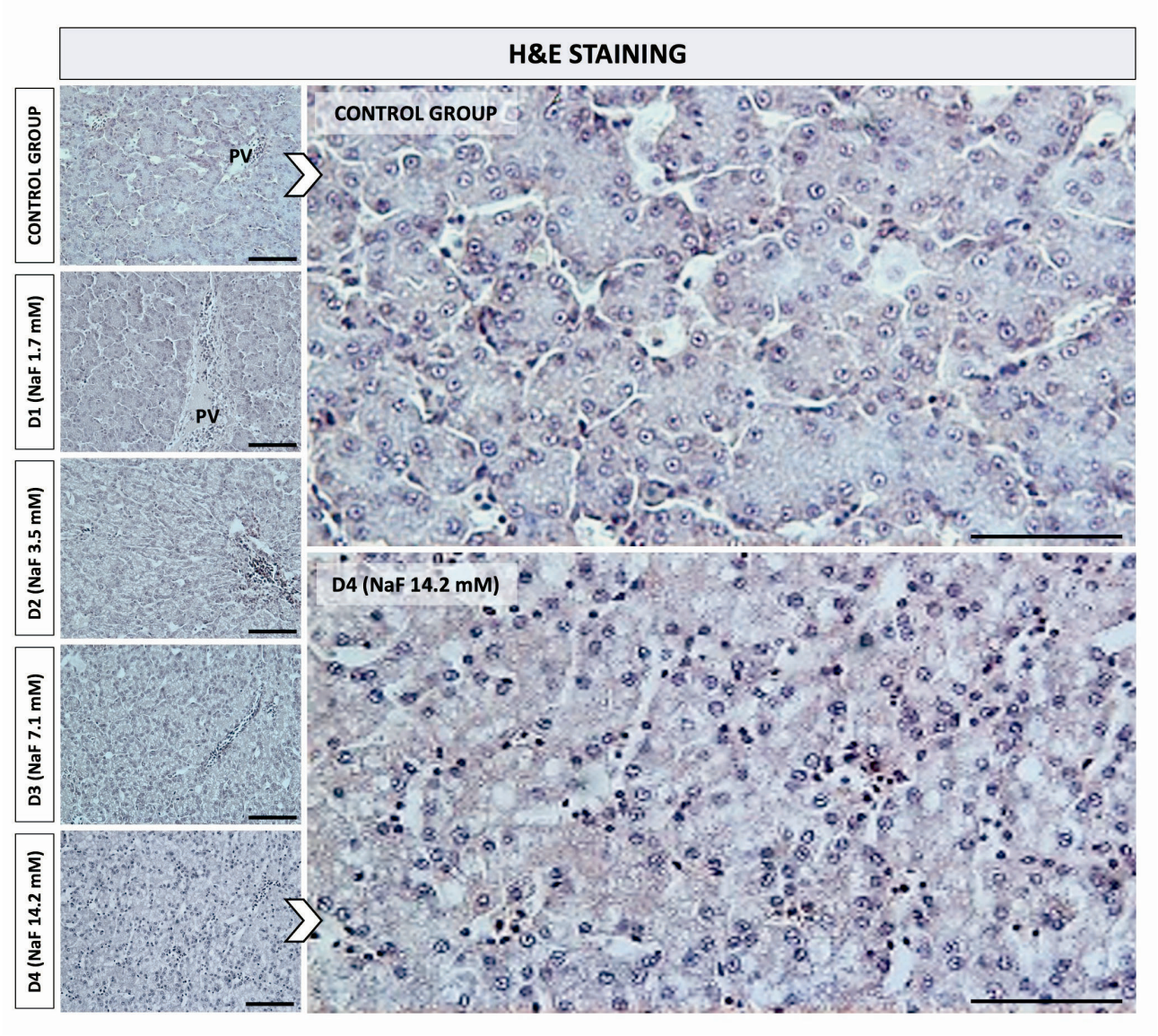

Fig. 2. Hematoxylin and Eosin staining in the liver tissues of chicken embryos in the control group and following an *in vitro* treatment with 1.7 (D1), 3.5 (D2), 7.1 (D3) and 14.2 mM (D4) NaF. Hematoxylin stains the cell nuclei a purplish blue, and eosin stains the extracellular matrix and cytoplasm pink, with the other structures taking on different shades, hues and combinations of these colours.

creased significantly in the D1 and D4 groups (Fig. 1 D). The expression of both analysed caspases (*CASP3* and *CASP9*) mRNA was significantly higher in the D1 group, as well as that of *CASP9* in the D3 group (Fig. 1E, F).

Histological analysis (Figs 2, 3)

In the NaF-treated livers stained with H&E, we observed a significant increase in the number of intracytoplasmic vacuoles and pyknotic nuclei, mainly in the experimental group where the highest dose of NaF was used (Fig. 2). Feulgen staining showed a dramatic increase in the number of early-apoptotic nuclei and apoptotic bodies in the group that was exposed to the highest NaF dose (D4) (Fig. 3).

Localisation of apoptotic cells

The number of apoptotic cells gradually increased in the NaF-treated groups, ranging from 18% in the control group to the highest value of 49% in the D4 group (Fig. 4). The highest numbers of TUNEL-positive cells were observed near the blood vessels. Perivascular cells, connective tissue cells as well as hepatocytes in the developing liver also showed a significantly higher signal in the D4 experimental group.

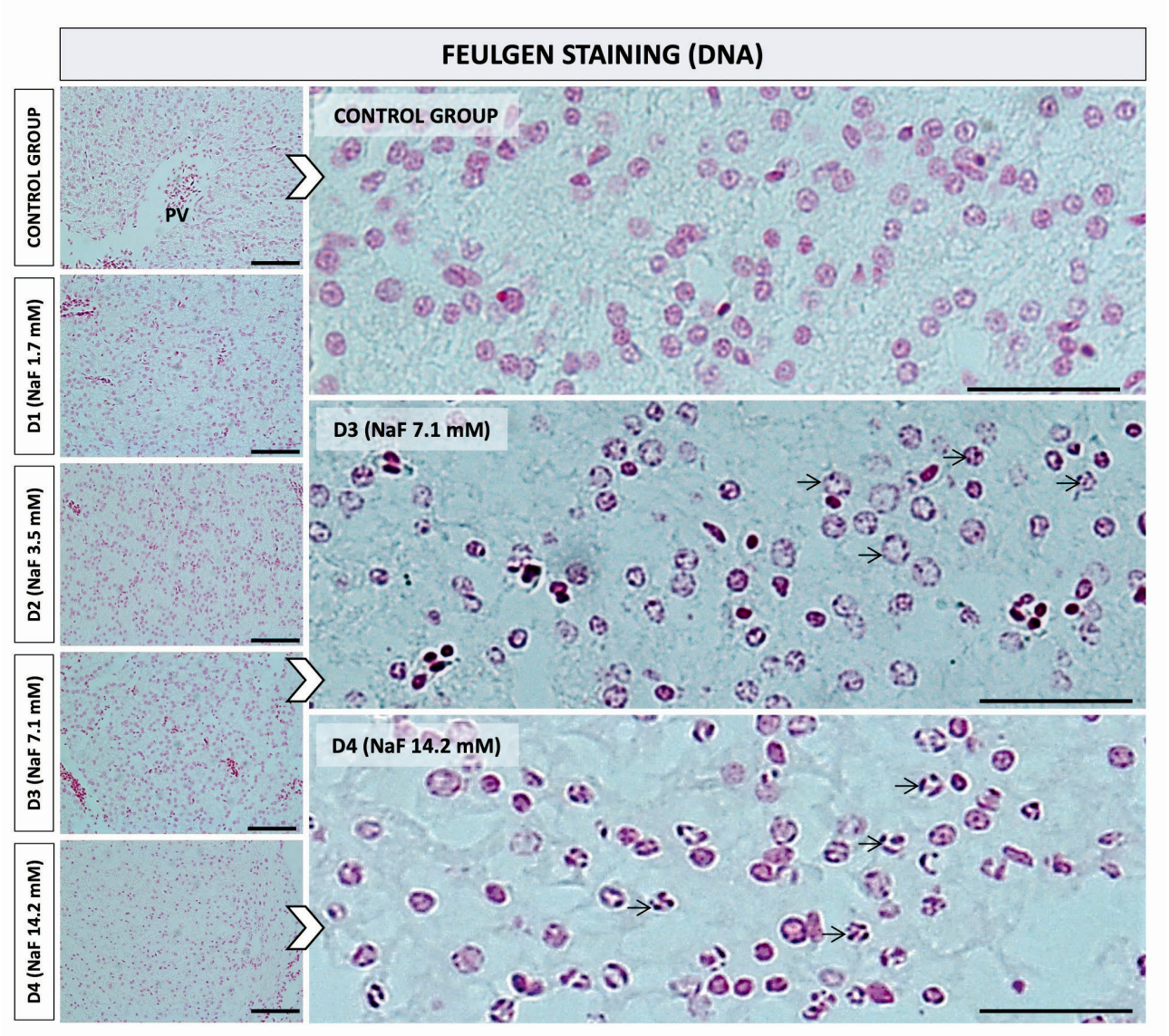

Fig. 3. Feulgen staining in the liver tissues of chicken embryos in the control group and following an *in vitro* treatment with 1.7 (D1), 3.5 (D2), 7.1 (D3) and 14.2 mM (D4) NaF. DNA – pink (magenta) staining.

Immunoexpression of CASP3 and APAF1

The expression of apoptosis regulatory factors increased as follows: CASP3 immunopositivity in the D3 and D4 groups was significantly more intensive in single cells in the embryonic liver (Fig. 5), whereas that of APAF1 in the D3 and D4 groups increased in the perivascular cells, and hepatocytes were localised mainly near the portal vein as well as the blood vessel walls (Fig. 6).

Localisation of proliferating cells (PCNA antigen)

The proliferating cell number decreased significantly in a dose-dependent manner, ranging from 84% in the control group to 53% in the D1 group, 35% in the D2 group, 19% in the D3 group and 5.5% in the D4 group (Fig. 7).

Discussion

In the present study, changes in the mRNA expression as well as in the immunolocalisation of apoptosis regulators after a treatment with NaF were observed in the livers of chicken embryos. In this experiment, four doses of NaF, ranging from 1.7 to 14.2 mM, were used (75-600 µg NaF/ml, i.e. per well). We did not observe a dose-dependent effect of the NaF-treatment on the mRNA expression of apoptosis regulators. However, this may have been a result of a very short time for the embryonic livers incubation. Phenotypic variability may also affect the adaptogenes expres-

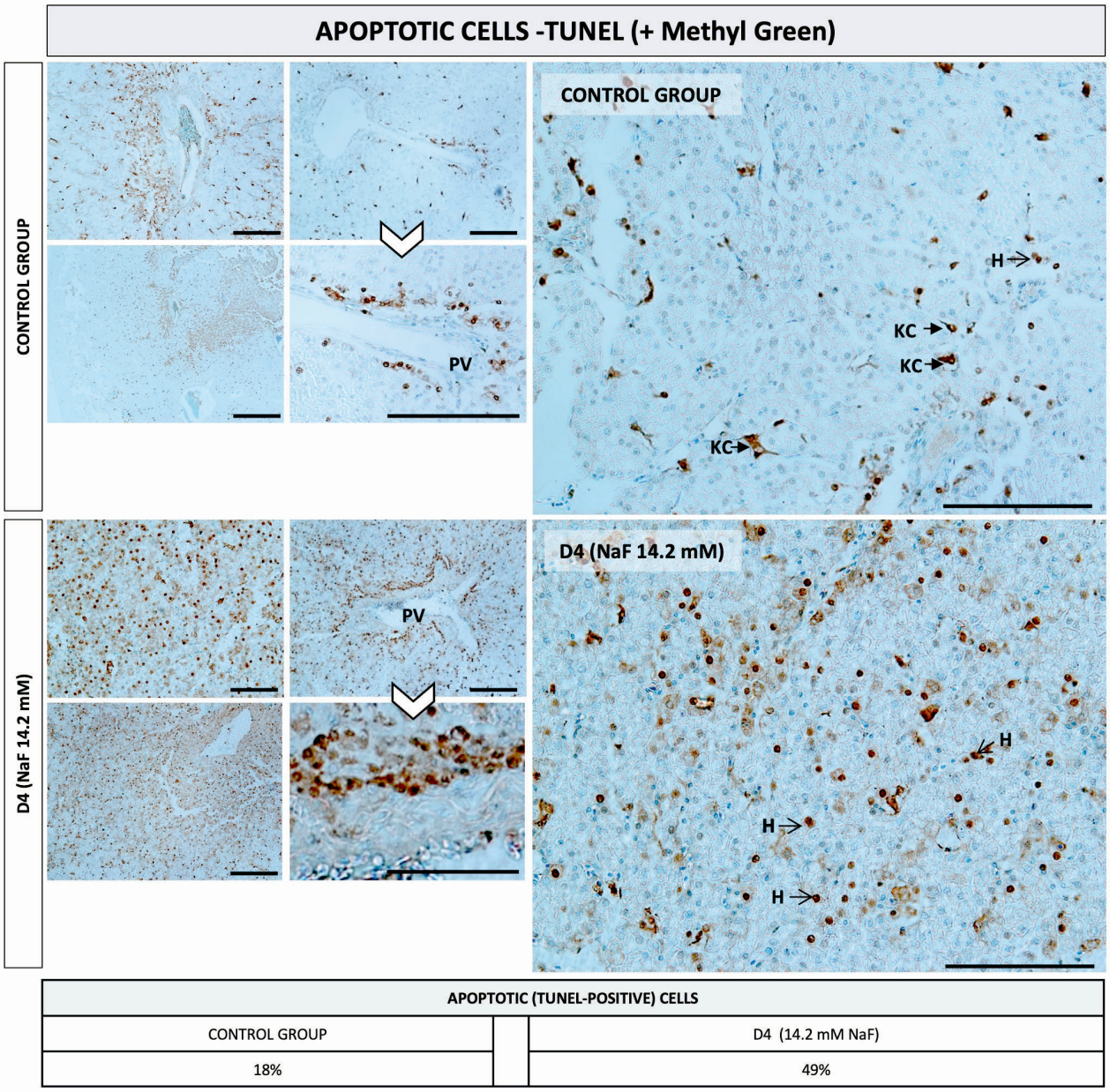

Fig. 4. Apoptotic cells detection by the TUNEL assay method in the liver tissues of chicken embryos in the control group and following an *in vitro* treatment with 14.2 mM (D4) NaF. Apoptotic cells – brown staining (arrows); H – Hepatocyte, KC – Kupffer Cells, PV – portal vein.

sion. The lowest D1 dose significantly affected the mRNA encoding proteins regulating the intrinsic pathway of apoptosis activation (*CYCS, APAF1, CASP3* and *CASP9*), but the mRNA expression of the antiapoptotic protein *BCL2* also increased in this group. Higher doses of NaF altered the mRNA expression of *APAF1* and *CASP9*. These results suggest that the lowest dose, 1.7 mM NaF, may affect liver cell apoptosis at the mRNA level. The mechanism of the NaF action may be associated with the mitochondrial pathway of apoptosis activation. A significant increase in the apoptotic index, with a clearly visible decrease in the number of proliferating cells, was also observed.

Previously, LU *et al.* (2017) showed that NaF may cause oxidative stress and apoptosis in the mouse liver. They observed histopathological lesions including: hepatocellular granular degeneration; vacuolar degeneration; and necrosis with karyorrhexis, karyolysis and hypochromatosis. Similar effects we observed in NaF-treated livers of embryonic chickens. They also detected a significant increase in the

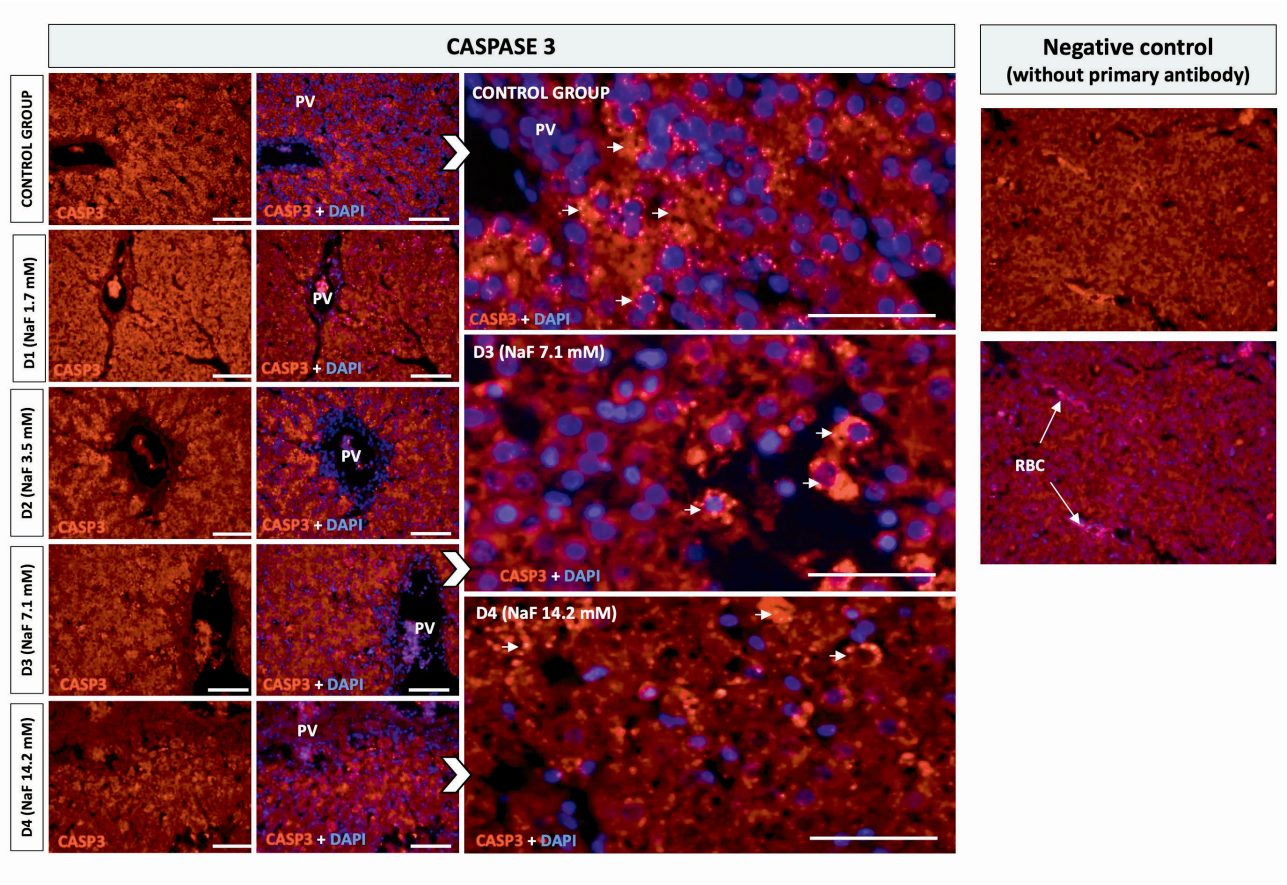

Fig. 5. Caspase-3 (CASP3) immunolocalisation in the liver tissues of chicken embryos in the control group and following an *in vitro* treatment with 1.7 (D1), 3.5 (D2), 7.1 (D3) and 14.2 mM (D4) NaF. Magnification 40x, and the scale bars represent 100 µm. The panels show a Caspase-3 immunopositive reaction (CASP3, red) and the merged images of DAPI and CASP3 staining (blue and red (arrows), respectively). Negative controls were incubated with a TBST buffer instead of the primary antibody; RBC – red blood cells.

mRNA expression of *CASP3* after 21 days, only in the group that was exposed to the highest NaF dose (48 mg/kg b.w.), and after 42 days in those groups exposed to doses of 12, 24 and 48 mg/kg. They observed more significant effects at the protein expression level (LU *et al.* 2017). In the present study, a significant increase in the mRNA expression of *CASP3* was observed only in the group that was exposed to the D1 NaF dose (1.7 mM). It is possible, in our experimental model, that this particle affects the protein rather than the mRNA expression after an incubation period of only 6 hours. In our study, significant increases in the apoptotic index and intensity of CASP3 and APAF1 immunopositivity, mainly in cells localised near the blood vessels, were observed in the groups exposed to the higher doses of NaF: 7.1 and 14.2 mM. In general, CASP3 is a key and common protease in both mitochondria- and death receptor-dependent pathways (EARNSHAW *et al.* 1999). The results of a study by LEE *et al.* (2008) showed that in human gingival fibroblasts, NaF increased the number of TUNEL-positive cells and induced apoptosis, with a concomitant chromatin condensation and DNA fragmentation. NaF has also a significant effect on MAP kinases, leading to the arrest of cell division, and as a result it may induce apoptosis processes in odontoblast-like cells (KARUBE *et al.* 2009).

The cell viability after a treatment with 5-40 mM of NaF for 12 h decreased from 100% to 11%. Approximately 60% of the cells survived an exposure to 20 mM NaF for 6 h. In addition, NaF increased the level of cytochrome c released from the mitochondria into the cytosol and enhanced the activities of CASP9, CASP8 and CASP3. An upregulation of Fas-ligand, a ligand of the death receptor in the NaF-treated group was also detected. BCL2, a member of the anti-apoptotic BCL2 family, was downregulated, whereas the expression of BAX, a member of the proapoptotic BCL2 family, was unaffected in the NaF-treated cells (LEE *et al.* 2008). In the embryonic chicken liver, we did not detect any differences in the mRNA expression of *TMBIM1*, which is an inhibitory apoptosis regulator in the receptor-dependent apoptosis induction pathway. This suggests that the intrinsic pathway

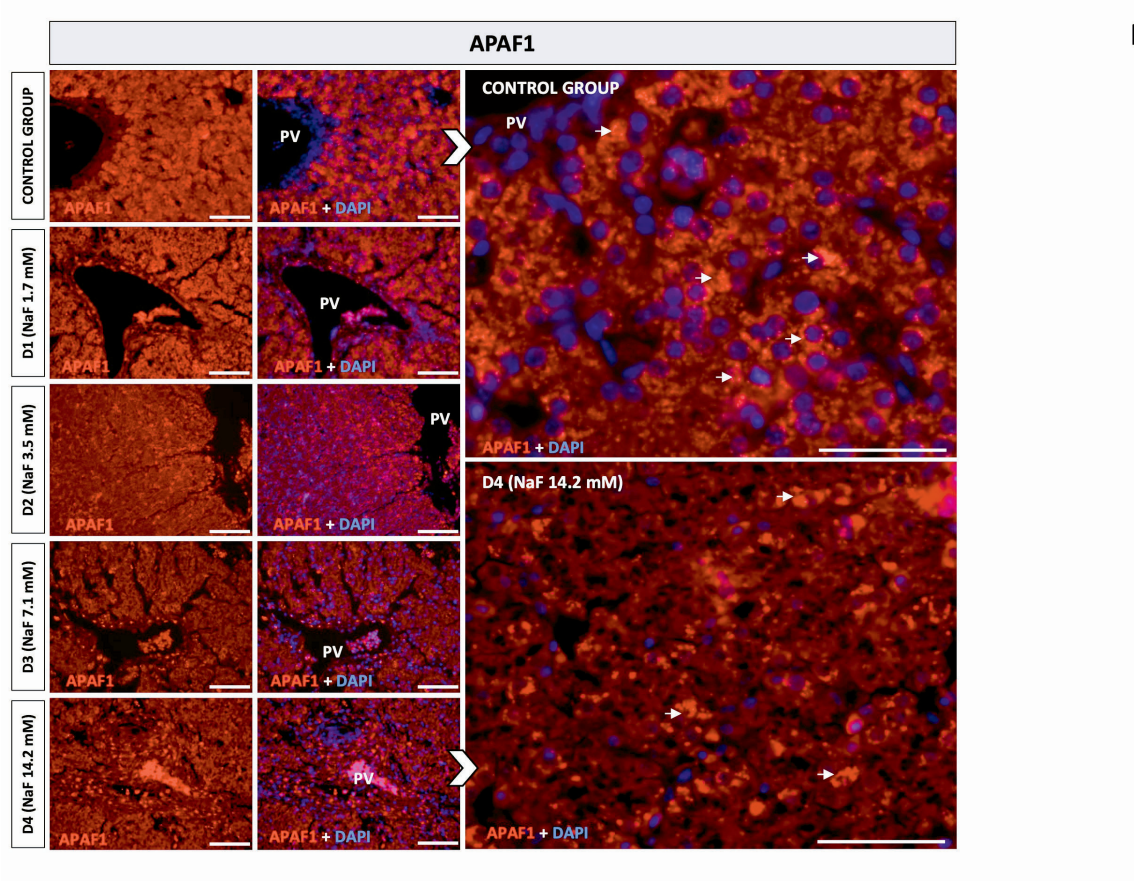

Fig. 6. APAF1 immunolocalisation in the liver tissues of chicken embryos in the control group and following an *in vitro* treatment with 1.7 (D1), 3.5 (D2), 7.1 (D3) and 14.2 mM (D4) NaF. Magnification 40x, and the scale bars represent 100 µm. The panels show an *APAF1* immunopositive reaction (APAF1, red) and the merged images of DAPI and APAF1 staining (blue and red (arrows), respectively).

of a programmed cell death is the main pathway affected by NaF in the liver of an embryonic chicken.

The mechanism of fluorine toxicity is very intricate. The high electronegativity of the F ion allows it to interact with both the organic and inorganic compounds of cells. Furthermore, fluorine is an anion with strong penetrability (ZHANG *et al.* 2016). It has a great affinity for the Ca^{2+}, Mg^{2+} and phosphate present in the culture medium and within cells, so the active agent could interfere with DNA polymerase and RNAase activities. The fluoride anion also forms a strong hydrogen bond with purine and pyrimidine bases, and may thus disrupt the structures of both DNA and RNA, and may interfere with their synthesis or enhance the frequency of base-pair errors during DNA replication. Fluoride has been found to inhibit protein synthesis and cell cycle progression (AARDEMA *et al.* 1989), and may also induce oxidative stress, which increases lymphocyte apoptosis (DENG *et al.* 2016).

In our study, a significant decrease in the proliferating index, accompanied by significant increases in the number of intracytoplasmic vacuoles and pyknotic nuclei, as well as a dramatic increase in the number of apoptotic nuclei and apoptotic bodies, was demonstrated in the group exposed to the highest NaF dose (D4). Previously, in a study with human osteosarcoma MG-63 cells as a model, it was shown that 5 mM of NaF may stimulate proliferation, whereas 20 mM of NaF inhibits cell proliferation and induces apoptosis (WEI *et al.* 2014). The results of an *in vitro* study by WANG *et al.* (2004) revealed that in normal human primary hepatocytes incubated with NaF (80 µg/ml) for 12 h, the number of cells significantly increased in the S phase, but the treatment had no effect on the cell numbers in the G0/G phase and G2/M phase. This finding indicates that fluoride can disturb signal transduction in the cell cycle and cause cell arrest in the S phase. HE & CHEN (2006) analysed the effect of fluoride, at a dose of 150 mg/l in drinking water for 4 weeks, on the cell cycle and proliferation index of oral mucosal cells and hepatocytes in rat specimens. Both the number of hepatocytes in the G0/G1, S and G2/M phases and the number of proliferating cells decreased. However, the apoptotic index increased sig-

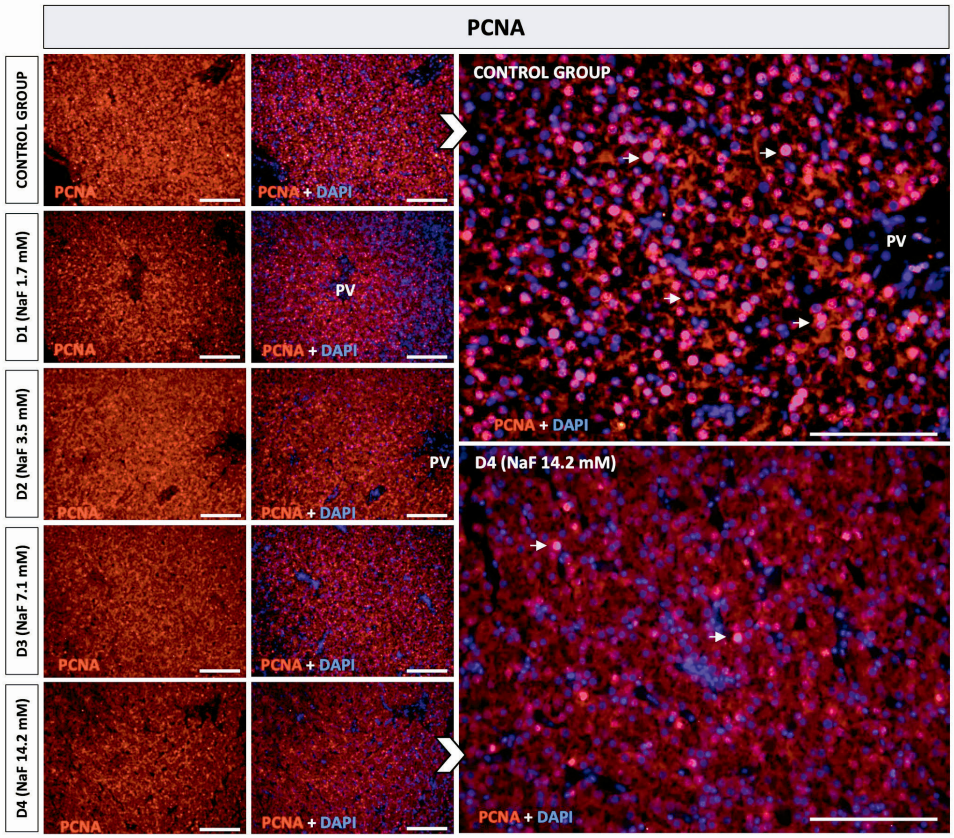

PROLIFERATING (PCNA - POSITIVE) CELLS				
CONTROL GROUP	D1 (1.7 mM NaF)	D2 (3.5 mM NaF)	D3 (7.1 mM NaF)	D4 (14.2 mM NaF)
84%	53%	35%	19%	5.5%

Fig. 7. PCNA immunolocalisation in the liver tissues of chicken embryos in the control group and following an *in vitro* treatment with 1.7 (D1), 3.5 (D2), 7.1 (D3) and 14.2 mM (D4) NaF. Magnification 40x, and the scale bars represent 100 µm. The panels show a PCNA immunopositive reaction (PCNA, red) and the merged images of DAPI and PCNA staining (blue and red, respectively).

nificantly (approximately 2-fold) in the NaF-treated group (HE & CHEN 2006).

Many studies have demonstrated that NaF may affect embryonic development. Previously, FU *et al.* (2016) showed that 1 mM of NaF did not significantly affect the proliferation of human embryonic stem cells, but disturbed the gene expression patterns of hESCs during embryonic differentiation. Higher doses of NaF (>2 mM) markedly decreased the viability and proliferation of these cells (FU *et al.* 2016), whereas the treatment of mouse embryonic stem cells with NaF doses greater than 1 mM reduced their viability and DNA synthesis, and induced cell cycle arrest in the G(2)/M phase as well as cell death, mainly by apoptosis rather than necrosis (NGUYEN NGOC *et al.* 2012). BAI *et al.* (2010) analysed the effect of fluoride on the renal cell population of chickens. They found that a fluoride treatment greatly increased the population of these cells in the early stage of apoptosis, and at higher doses, also increased the population of renal cells in end-stage apoptosis. These results suggest that a high dietary F intake (400-1200 mg F/kg) causes G0/G1 arrest and induces apoptosis of the renal cells in chickens, which likely influences the excretion and retention of fluoride in the body.

Our results reveal that NaF, by changing the balance between apoptosis and the proliferation of hepatocytes, may disturb the development and function of the liver in embryonic chickens. The World Health Organization (WHO) states that the reference range for fluoride in drinking water is 0.5-1.5 mg/l (FAWELL *et al.* 2006). The American Environmental Protection Association (EPA) and the American Public Health Service (PHS) previously reported the level of fluoride in drinking water to be 0.7-1.2 mg/l, while the PHS revised its optimal value to 0.7 mg/l (USA, EPA Regulations). The EPA states that there is no need for a reference update for the time being, but it will continue to follow up on the research conducted on this subject and refer to the reference regulation

when necessary (KIRMIT *et al.* 2020). The risk of exposure to NaF should be considered when determining the standards for human and animal exposure to this compound, and the chicken embryo may be used as an animal model to analyse the mechanisms of toxicity of NaF. Most of the literature data shows that the toxicity of fluoride is extremely dangerous for developing organisms. It should be emphasised that the chicken embryo is included in the inexpensive, generally available, alternative research models, and that research with the use of chicken embryos is recommended and complies with the guidelines of ethical committees. The individual development stages of a domestic chicken embryo are very well known and described, which is an additional advantage of this model.

Author Contributions

Research concept and design: A.K.G.; Collection and/or assembly of data: A.K.G., K.J.; Data analysis and interpretation: A.K.G., A.S., D.W., K.J.; Writing the article: A.K.G.; Critical revision of the article: A.S., D.W.; Final approval of article: A.S.

Conflict of Interest

The authors declare no conflict of interest.

Financial support statement

This work received financial support from the National Science Centre, Poland (Grant MINIATURA No. 2017/01/X/NZ8/00094) dedicated to A. GRZEGORZEWSKA.

References

AARDEMA M.J., GIBSON D.P., LE BOEUF R.A. 1989. Sodium fluoride induced chromosome aberrations in different stages of the cell cycle: a proposed mechanism. Mutat. Res. Genetic Toxicol. Environ. Mutagenesis. **223**: 191-203. https://doi.org/10.1016/0165-1218(89)90047-5

BAI C., CHEN T., CUI Y., GONG T., PENG X., CUI H.M. 2010. Effect of high fluorine on the cell cycle and apoptosis of renal cells in chickens. Biol. Trace Elem. Res. **138**: 173-180. https://doi.org/10.1007/s12011-009-8599-z

CAO J., CHEN J., XIE L., WANG J., FENG C., SONG J. 2015. Protective properties of sesamin against fluoride-induced oxidative stress and apoptosis in kidney of carp (*Cyprinus carpio*) via JNK signaling pathway. Aquat. Toxicol. **167**: 180-190. https://doi.org/10.1016/j.aquatox.2015.08.004

DENG H., KUANG P., CUI H., LIAN CHEN L., LUO Q., FANG J., ZUO Z., DENG J., WANG X., ZHAO L. 2016. Sodium fluoride (NaF) induces the splenic apoptosis via endoplasmic reticulum (ER) stress pathway *in vivo* and *in vitro*. Aging (Albany NY) **8**: 3552-3567. https://doi.org/10.18632/aging.101150.

EARNSHAW W.C., MARTINS L.M., KAUFMANN S.H. 1999. Mammalian caspases: structure, activation, substrates, and functions during apoptosis. Annu. Rev. Biochem. **68**: 383-424. https://doi.org/10.1146/annurev.biochem.68.1.383

EKERT P.G., SILKE J., HAWKINS C.J., VERHAGEN A.M., VAUX D.L. 2001. DIABLO promotes apoptosis by removing MIHA/XIAP from processed caspase 9. J. Cell Biol. **152**: 483-490. https://doi.org/10.1083/jcb.152.3.483.

EKSTRAND J., KOCH G., LINDGREN L.E., PETERSSON L.G. 1981. Pharmacokinetics of fluoride gels in children and adults. Caries Res. **15**: 213-220. https://doi.org/10.1159/000260517

ELWAN H., XIE C., MIAO L.P., DONG X., ZOU X.T., MOHANY M., AHMED M.M., AL-REJAIE S.S., ELNESR S.S. 2021. Methionine alleviates aflatoxinb1-induced broiler chicks embryotoxicity through inhibition of caspase-dependent apoptosis and enhancement of cellular antioxidant status. Poultry Sci. **100**: 101103. https://doi.org/10.1016/j.psj.2021.101103

EPA (United States Environmental Protection Agency): Review of the Fluoride Drinking Water Regulation. Available from: https://www.epa.gov/dwsixyearreview/review fluoridedrinking-water-regulation

FAWELL J., BAILEY K., CHILTON J., DAHI E., MAGARA Y. 2006. Fluoride in Drinking water: The International Water Association Publishing.

FORDYCE F.M. 2011. Fluoride: human health risks. Encyclopedia of environmental health **5**: 776-785.

FRENI S.C. 1994. Exposure to high fluoride concentrations in drinking water is associated with decreased birth rates. J. Toxicol. Environ. Health **42**: 109-121. https://doi.org/10.1080/15287399409531866

FU X., XIE F.N., DONG P., LI Q.C., YU G.Y., XIAO R. 2016. High-Dose Fluoride Impairs the Properties of Human Embryonic Stem Cells via JNK Signaling. PLoS One 11, e0148819. https://doi.org/10.1371/journal.pone.0148819

GAVRIELI Y., SHERMAN Y., BEN-SASSON S.A. 1992. Identification of programmed cell death *in situ* via specific labeling of nuclear DNA fragmentation. J. Cell Biol. **119**: 493-501. https://doi.org/10.1083/jcb.119.3.493

GRIFFIN S.O., REGNIER E., GRIFFIN P.M., HUNTLEY V. 2007. Effectiveness of fluoride in preventing caries in adults. J. Dent. Res. **86**: 410-415. https://doi.org/10.1177/154405910708600504

GRZEGORZEWSKA A.K. 2020. Assessment of follicle-stimulating hormone (FSH)-, luteinizing hormone (LH)-, estrogen (α and β)- and progesterone (PR) receptors mRNA expression in the gonads and liver of chicken (*Gallus domesticus*) embryo. Rocz. Nauk. Zoot. **47**: 87-97.

GRZEGORZEWSKA A.K., HRABIA A., KOWALIK K., KATARZYŃSKA-BANASIK D., KOZUBEK A., SECHMAN A. 2020a. *In vitro* effects of PNP and PNMC on apoptosis and proliferation in the hen ovarian stroma and prehierarchal follicles. Acta Histochem. **122**: 151463. https://doi.org/10.1016/j.acthis.2019.151463

GRZEGORZEWSKA A.K., OCŁOŃ E., KUCHARSKI M., SECHMAN A. 2020b. Effect of *in vitro* sodium fluoride treatment on CAT, SOD and Nrf mRNA expression and immunolocalisation in chicken (*Gallus domesticus*) embryonic gonads. Theriogenology **157**: 263-275. https://doi.org/10.1016/j.theriogenology.2020.07.020

GUAN Z.Z., XIAO K.Q., ZENG X.Y., LONG Y.G., CHENG Y.H., JIANG S.F., WANG Y.N. 2000. Changed cellular membrane lipid composition and lipid peroxidation of kidney in rats with chronic fluorosis. Arch. Toxicol. **74**: 602-608. https://doi.org/10.1007/s002040000177

GUNA SHERLIN D.M., VERMA R.J. 2001. Vitamin D Ameliorates fluoride-induced embryotoxicity in pregnant rats. Neurotoxicol. Teratol. **23**: 197-201. https://doi.org/10.1016/s0892-0362(00)00123-9

GUPTA R.S., KHAN T.I., AGRAWAL D., KACHHAWA J.B. 2007. The toxic effects of sodium fluoride on the reproductive system of male rats. Toxicol. Ind. Health 23: 507-513. https://doi.org/10.1177/0748233708089041.

HAO Y., LIU J., FENG Y., YU S., ZHANG W., LI L., MIN L., ZHANG H., SHEN W., ZHAO Y. 2017. Molecular evidence of offspring liver dysfunction after maternal exposure to zinc oxide nanoparticles. Toxicol. Appl. Pharmacol. **329**: 318-325. https://doi.org/10.1016/j.taap.2017.06.021

HE L.F., CHEN J.G. 2006. DNA damage, apoptosis and cell cycle changes induced by fluoride in rat oral mucosal cells and hepatocytes. World J. Gastroenterol. **12**: 1144-1148. https://doi.org/10.3748/wjg.v12.i7.1144

HIRATA M., HALL B. 2000. Temporospatial patterns of apoptosis in chick embryos during the morphogenic period of development. Int. J. Dev. Biol. **44**: 757-768.

KARUBE H., NISHITAI G., INAGEDA K., KUROSU H., MATSUOKA M. 2009. NaF activates MAPKs and induces apoptosis in odontoblast-like cells. J. Dent. Res. **88**: 461-465. https://doi.org/10.1177/0022034509334771

KHILLARE G.S., SASTRY K.V.H., AGRAWAL R., SAXENA R., MOHAN J., SINGH R.P. 2018. Expression of gonadotropin and sex steroid hormone receptor mRNA in the utero-vaginal junction containing sperm storage tubules of oviduct during sexual maturation in Japanese quail. Gen. Comp. Endocrinol. **259**: 141-146. https://doi.org/10.1016/j.ygcen.2017.11.015

KIRMIT A., YESILNACAR M., CALISIR M., BAYHAN I., CELIK H., 2020. Oxidative stress, DNA damage and apoptosis levels in those who use borderline high level fluoride content drinking water. J. Contemp. Med. **10**: 45-50. https://doi.org/10.16899/jcm.690968

LAHIJANI M.S., FARIVAR S., KHODAEIAN M. 2011. Effects of 50 Hz electromagnetic fields on the histology, apoptosis, and expression of c-Fos and β-catenin on the livers of preincubated white Leghorn chicken embryos. Electromagn. Biol. Med. **30**: 158-169. https://doi.org/10.3109/15368378.2011.596603

LANTZ O., JOUVIN M.H., DE VERNEJOUL M.C., DRUET P. 1987. Fluoride-induced chronic renal failure. Am. J. Kidney Dis. **10**: 136-139.

LEE J.H., JUNG J.Y., JEONG Y.J., PARK J.H., YANG K.H., CHOI N.K., KIM S.H., KIM W.J. 2008. Involvement of both mitochondrial- and death receptor-dependent apoptotic pathways regulated by Bcl-2 family in sodium fluoride-induced apoptosis of the human gingival fibroblasts. Toxicology **243**: 340-347. https://doi.org/10.1016/j.tox.2007.10.026

LIVAK K.J., SCHMITTGEN T.D. 2001. Analysis of Relative Gene Expression Data Using Real-Time Quantitative PCR and the 2–ΔΔCT Method. Methods **25**: 402-408. https://doi.org/10.1006/meth.2001.1262

LU Y., LUO Q., CUI H., DENG H., KUANG P., LIU H., FANG J., ZUO Z., DENG J., LI Y., WANG X., ZHAO L. 2017. Sodium fluoride causes oxidative stress and apoptosis in the mouse liver. Aging (Albany NY) **9**: 1623-1639. https://doi.org/10.18632/aging.101257

MELLO M.L.S., VIDAL B.C. 2017. The Feulgen reaction: A brief review and new perspectives, Acta Histochem. **119**: 603-609. https://doi.org/10.1016/j.acthis.2017.07.002

NGUYEN NGOC T.D., SON Y.O., LIM S.S., SHI X., KIM J.G., HEO J.S., CHOE Y., JEON Y.M., LEE J.C. 2012. Sodium fluoride induces apoptosis in mouse embryonic stem cells through ROS-dependent and caspase and JNK-mediated pathways. Toxicol. Appl. Pharmacol. **259**: 329-337.

ROJAS-RIVERA D., HETZ C. 2015. TMBIM protein family: ancestral regulators of cell death. Oncogene **34**: 269-280. https://doi.org/10.1038/onc.2014.6

SHIVASHANKARA A.R., SHIVARAJASHANKARA Y.M., PERUMUNDA B., SUDHA H.R. 2000. A clinical and biochemical study of chronic fluoride toxicity in children of Kheru Thanda of Gulbarga district, Karnataka, India. Fluoride **33l**: 66-73.

STRASSER A., NEWTON K. 1999. FADD/MORT1, a signal transducer that can promote cell death or cell growth. Int. J. Biochem. Cell Biol. **31**: 533-537. https://doi.org/10.1016/s1357-2725(99)00003-5

WANG A.G., XIA T., RU R., YUAN J., CHEN X.M., YANG K.D. 2004. Antagonistic effect of selenium on oxidative stress, DNA damage, and apoptosis induced by fluoride in human hepatocytes. Fluoride **37**: 107-116.

WEI Y., WU Y., ZENG B., ZHANG H. 2014. Effects of sodium fluoride treatment *in vitro* on cell proliferation, BMP-2 and BMP-3 expression in human osteosarcoma MG-63 cells. Biol. Trace Elem. Res. **162**: 18-25. https://doi.org/10.1007/s12011-014-0148-8

XIONG X., LIU J., HE W., XIA T., HE P., CHEN X., YANG K., WANG A. 2007. Dose-effect relationship between drinking water fluoride levels and damage to liver and kidney functions in children. Environ. Res. **103**: 112-116. https://doi.org/10.1016/j.envres.2006.05.008

YIN S., CUI H., PENG X., FANG J., ZUO Z., DENG J., WANG X., WU B., GUO H. 2016. Toxic effect of NiCl2 on development of the bursa of Fabricius in broiler chickens Oncotarget **7**: 125-139. https://doi.org/10.18632/oncotarget.6591

ZHANG J., LI Z., QIE M., ZHENG R., SHETTY J., WANG J. 2016. Sodium fluoride and sulfur dioxide affected male reproduction by disturbing blood-testis barrier in mice. Food Chem. Toxicol. **94**: 103-111. https://doi.org/10.1016/j.fct.2016.05.017